



## Tunable dual-band terahertz metalens based on stacked graphene metasurfaces

Zhiping Yin <sup>a,b</sup>, Qun Zheng <sup>a,b</sup>, Kuiyuan Wang <sup>a</sup>, Kai Guo <sup>c</sup>, Fei Shen <sup>c</sup>, Hongping Zhou <sup>c</sup>, Yongxuan Sun <sup>c</sup>, Qingfeng Zhou <sup>c</sup>, Jun Gao <sup>c</sup>, Linbao Luo <sup>a</sup>, Zhongyi Guo <sup>a,b,c,d,\*</sup>

<sup>a</sup> School of Electronics Science and Applied Physics, Hefei University of Technology, Hefei, 230009, China

<sup>b</sup> School of Instrument Science and Opto-electronics Engineering, Hefei University of Technology, Hefei, 230009, China

<sup>c</sup> School of Computer and Information, Hefei University of Technology, Hefei, 230009, China

<sup>d</sup> State Key Laboratory of Millimeter Waves, Southeast University, Nanjing 210096, China

### ARTICLE INFO

#### Keywords:

Graphene  
Metasurface  
Focusing lens  
Multifunctional device

### ABSTRACT

In this paper, we propose and theoretically investigate a tunable stacked graphene metasurface, which can independently manipulate electromagnetic field at different terahertz frequency. By tuning the Fermi levels of graphene ribbons, the designed two-layers graphene ribbons can realize a required phase shift of  $\sim 2\pi$  for manipulating the terahertz wavefronts owing to the excitation of plasmon resonances at each layer of graphene ribbons. A reflective double-frequencies focusing metalens has been designed working at 3.5 THz and 7.0 THz. For the designed lens with focal lengths of 300  $\mu\text{m}$ , the focus depth of 3.5 THz and 7.0 THz electromagnetic wave (full width at half maximum along the Z direction) is 174.7  $\mu\text{m}$  and 84  $\mu\text{m}$ , respectively. In addition, the resolution of focal points (full width at half maximum along the X direction) are close to the half-wavelength in the focusing plane, which are 48.2  $\mu\text{m}$  and 21.5  $\mu\text{m}$  respectively, demonstrating that the proposed metalens has superior performance. Furthermore, the focal length and offset distance of focal point of the lens can be tuned actively by changing gate voltages. The present graphene metasurface paves the way to engineering various potential applications for tunable, multiband, multifunctional metasurfaces.

### 1. Introduction

Metasurfaces are a new class of quasi 2D metamaterials that provide fascinating capabilities for manipulating light in an ultrathin scale. Compared to bulk metamaterial, metasurface has lower loss and is easier to fabricate. By tailoring the morphology, plasmonic and dielectric metasurface can support surface plasmon and Mie resonances, respectively, providing a unique opportunity to artificially control phase, amplitude and polarization of light [1–4]. Therefore, metasurfaces are promising for novel device applications, such as anomalous refraction [1,5], surface plasmon [6–8], ultrathin flat lens [9–11], polarization beam splitters [12,13] and cross polarization converters [14,15].

However, once the metasurfaces are designed, their working frequencies are fixed in a narrow range, especially for metasurface based on resonances with high quality. This feature of metasurface hinders its practical application in broadband response and tunability. To overcome this drawback, great efforts have been made to achieve tunable metasurfaces. One direct way to realize the active control is to construct metasurface by using materials with tunable optical response [16,17].

Therefore, the optical response of the metasurface can also be actively controlled by external stimulus such as electric, chemical doping or temperature.

Graphene is a monolayer of hexagonally arranged carbon atoms and has been demonstrated to support the surface plasmon polaritons at terahertz frequency ranges with lower loss compared to noble metal [18,19]. In addition, its Fermi level can be electrically and chemically tuned, thereby determining its optical response [20–22]. These advantages of graphene make it a good candidate for constructing the novel tunable metasurface. On the other hand, graphene is almost transparent when there is no resonance taken place in it. This provides the possibility of realizing multifunctional and multiband devices by using graphene. The usual solution is to utilize a planar multiplexing design that implements multifunction and multiband devices by combining different sets of resonators at different target frequencies. Particularly, for graphene metasurfaces, in addition to changing its geometry, the Fermi level of each individual resonator can be individually adjusted to interact light with different frequencies. Recently, Liu et al. designed a metasurface

\* Corresponding author.

E-mail addresses: [lbluo@hfut.edu.cn](mailto:lbluo@hfut.edu.cn) (L. Luo), [guozhongyi@hfut.edu.cn](mailto:guozhongyi@hfut.edu.cn) (Z. Guo).

that can effectively focus terahertz waves from 1.2 to 1.9 THz to the same focal point by changing the Fermi level of each graphene resonator separately [23]. Ma et al. have realized  $2\pi$  phase modulation by tuning the width of graphene ribbons and designed a dual-band focusing reflector operating at 25 THz and 16 THz [24]. Nevertheless, these designs are working for one frequency or accomplished by adjusting the width of each graphene ribbon and cannot be flexibly regulated. It is impossible to flexibly adjust the operating frequency and focal length in practical applications for multifunctional devices.

In this paper, we design a flexibly tunable metasurface by using stacked graphene that composed of two layer of graphene ribbons. Different from traditional devices, the designed device can cover a nearly  $2\pi$  phase region by adjusting the gate voltage to change the Fermi level of each layer of graphene ribbons. On the other hand, the interaction between two layers of graphene will be diminished since their working frequencies are far enough. As a result, we achieve a dynamically controlled dual-band stacked graphene metasurface by tuning the gate voltages. Here, a reflective focusing lenses is designed to work at frequencies of 3.5 THz and 7 THz. It is demonstrated that the position of focus can be arbitrarily adjusted with the focusing points either along or away from the device symmetry axis. Our results show that the designed stacked graphene metasurface has great potential for multifunctional and multiband devices in the terahertz and infrared regions.

## 2. Structure and result discussion

Fig. 1 schematically shows the proposed stacked graphene metasurface in. An Ag layer acts as a rear reflector, and four alternating layers of dielectric and graphene ribbons are stacked sequentially on top of the Ag reflector. The different Fermi levels can be achieved by tuning the gate voltages. The cross-sectional view of a unit cell of the designed structure is shown in Fig. 1(b). The period and width of graphene ribbons is  $P = 5 \mu\text{m}$  and  $w = 2.9 \mu\text{m}$ , respectively. The thicknesses of two dielectric layers are set as  $d_2 = 8 \mu\text{m}$ ,  $d_1 = 13.8 \mu\text{m}$ , and their refractive index is  $n = 1.45$ . The Ag layer is set as optical thick  $d_3 = 2 \mu\text{m}$  at the bottom serving as the perfect reflector to eliminate transmission. Since graphene ribbons and the Ag layer act as the reflecting mirror on both sides, Fabry–Perot resonance occurs in the dielectric spacer layer, which can increase the interactions between the graphene and the incident light. By separately considering each layer of the graphene ribbon, the incident wave will be strongly coupled with one of them and weakly interacted with the other one. Therefore, two graphene layers can control incident light independently by tuning Fermi levels of each layer of graphene ribbons. In experiments, the Ag film can be deposited on the substrate by electron beam evaporation system, which can be used as the electrodes [25,26]. Then, the dielectric layer (SiO<sub>2</sub>) can be deposited on the Ag film by using plasma enhanced chemical vapor deposition (PECVD), which take advantage to the reaction between the SiH<sub>4</sub> and N<sub>2</sub>O in the state of plasma. The single-layer graphene can be transferred to the dielectric layer, and graphene nanoribbon can be patterned by using electron-beam lithography, which can be used as electrode to apply the gate voltage as shown in Fig. 1(b) [25,26]. Lastly, by repeating the progress, the stacked graphene metasurface can be achieved.

As we all knows, optical response of graphene is characterized by the surface conductivity  $\sigma(\omega)$ , consisting of intraband electron–photon scattering and the interband transition contribution. It can be referred following the Kubo formula [27–29]:

$$\sigma_g = -\frac{ie^2(\omega + i\tau^{-1})}{\pi\hbar^2} \left[ \int_{-\infty}^{+\infty} \frac{|\epsilon|}{\omega + i\tau^{-1}} \frac{\partial f_d(\epsilon)}{\epsilon} d\epsilon - \int_0^{+\infty} \frac{\partial f_d(-\epsilon) - \partial f_d(\epsilon)}{(\omega + i\tau^{-1})^2 - 4(\epsilon/\hbar^2)^2} d\epsilon \right] \quad (1)$$

where  $f_d = 1/(1 + \exp[(\epsilon - \mu_c)/k_B T])$  is the Fermi–Dirac distribution,  $k_B$  is the Boltzmann constant,  $\epsilon$  is the energy,  $\mu_c$  is the chemical

potential,  $e$  is the electron charge,  $\hbar$  is the reduced Planck's constant, and  $\tau$  stands for the momentum relaxation time due to charge carrier scattering. At room temperature, the chemical potential (Fermi level) is very close to Fermi energy [30]. In the following, we will replace the chemical potential  $\mu_c$  with the Fermi level  $E_f$ . In the terahertz region, the intraband contribution is dominant in the heavily-doped graphene because  $E_f \gg \hbar\omega \gg k_B T$ , so that  $\sigma(\omega)$  can be further simplified [31,32]:

$$\sigma_g(\omega) = ie^2 E_f / [\pi\hbar^2 (\omega + i/\tau)] \quad (2)$$

In general, the relation between momentum relaxation time  $\tau$ , the carrier mobility  $\mu$ , the Fermi level  $E_f$ , and the Fermi velocity  $v_f$  can be expressed as  $\tau = \mu E_f / e v_f^2$ , which indicates that increase of carrier mobility in graphene will reduce the loss and improve the device efficiency effectively. Here, the Fermi velocity  $v_f$  is set as  $10^6$  m/s, and the carrier mobility  $\mu$  is set as  $40\,000 \text{ cm}^2/\text{Vs}$ , which can be achieved in experiment [33]. The Fermi levels in graphene can be expressed as  $E_f = \hbar v_f (\pi n_s)^{1/2}$ . The doping level of graphene  $n_s$  shows a linear dependence on the external gate voltage described as  $n_s = \epsilon_p \epsilon_0 V_b / (eh)$  [34]. The  $\epsilon_p$  and  $V_b$  are the relativity permittivity of the dielectric layer and external voltage, respectively. Thus, the gate voltage can effectively change the Fermi levels and surface conductivity of the graphene. By treating the graphene monolayer as an ultra-thin metal film, the permittivity [35] of graphene can be modeled as follow:

$$\epsilon_g = 1 + \frac{i\sigma_g}{\epsilon_0 \omega t} \quad (3)$$

where  $\epsilon_0$  is the vacuum permittivity,  $t$  is set as 0.35 nm that is the graphene thickness [36]. As a result, the optical responses of graphene can be flexibly tuned by changing Fermi level of graphene ribbons.

In our study, the graphene ribbon is regarded as an electric dipole that can introduce realize effective modulations of amplitude and phase of the reflected wave. Combining with Fabry–Perot resonance in the dielectric interlayer, the phase-shift of the reflective waves can cover nearly  $2\pi$  range. The wave vector of surface plasmons along the graphene metasurface satisfies the expression of  $\kappa_{spp} = \hbar\omega_r / 2\epsilon_0 \alpha_0 E_f$  [37], where  $\omega_r$  is the resonant angular frequency,  $\alpha_0 = e^2 / \hbar c$  is the fine structure constant [38]. After transformation, the resonant frequency  $f_r$  can be expressed as [39]:

$$f_r = \sqrt{\alpha_0 E_f / 2\pi^2 \hbar c L_s} \propto \sqrt{E_f / L_s} \quad (4)$$

where the resonant length  $L_s$  associated with the structural parameters. According to the expression, the resonant frequency of  $f_r$  is proportional to  $\sqrt{E_f}$ . Based on this model, the working frequency and Fermi level can be chosen properly. To understand the physical mechanism of the stacked graphene metasurface, a homemade software based on finite element method is used to simulate the phase shift and reflectance of the metasurface.

Usually, the interaction between light and graphene is very weak because graphene has only one carbon atomic thickness. It is a common disadvantage for most optoelectronic devices. But in our proposed devices, the stacked graphene takes full advantage of this feature to achieve multi-band devices. At a specific resonant frequencies, the corresponding graphene ribbon works as a predefined function, and for the other graphene layer, its interaction with light is quite weak, which make graphene be almost transparent. Therefore, we can separate the optical response of two layers of graphene ribbons at different frequencies of incident light and there is not interfering with each other in response to different target frequencies, which is actually difficult by using the stacked metal structure. However, the resonant frequencies of both layers of graphene ribbons can be independently tuned by Fermi levels ranging in 0–1 eV. Therefore, we should choose the appropriate resonant frequencies to separate the Fermi levels of the corresponding resonances to reduce the interaction between two layers of graphene ribbon. According to Eq. (4), we choose the working frequency of the metasurfaces as 3.5 THz and 7.0 THz.

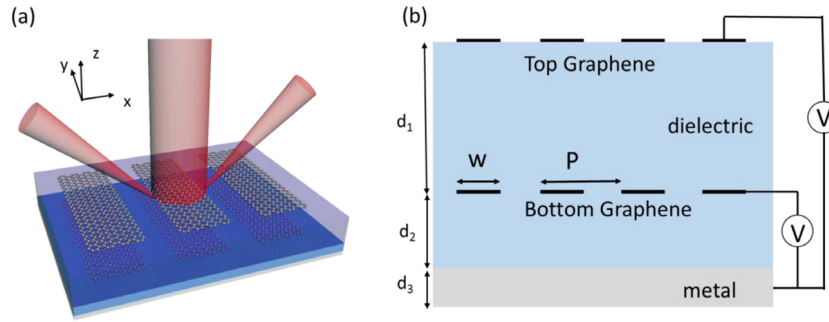


**Fig. 1.** (a) Schematic of the stacked graphene plasmonic metasurface structure. (b) The cross-sectional view of the stacked graphene plasmonic metasurface.  $P$  is the grating period, and  $w$  denotes the widths of graphene ribbons.  $d_1$ ,  $d_2$  and  $d_3$  are the thickness of dielectric layer and Ag layer, respectively.

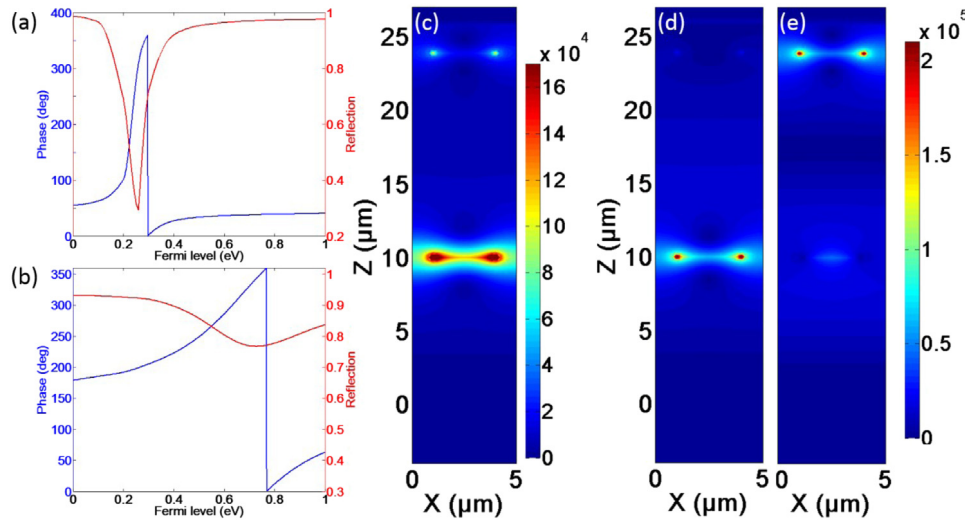


**Fig. 2.** Reflectance and phase shift as the functions of Fermi levels at the frequencies of (a) 3.5 THz and (b) 7.0 THz. Intensity distributions of electric field at the frequencies of 3.5 THz (c) with the same Fermi level of 0.26 eV, and at 3.5 THz (d) and (e) 7.0 THz with different Fermi levels of 0.26 eV and 0.73 eV, respectively.

Fig. 2(a) and (b) shows the dependence of reflective response of the proposed structure on Fermi level at 3.5 THz and 7.0 THz, respectively. It is clear that the resonant characteristics appear at 0.26 eV and 0.73 eV, presenting dramatic change of the reflection amplitude and phase. In addition, the relation of reflectance, phase and frequency with Fermi level in Fig. 2(a) and (b) agrees well with Eq. (4). Meanwhile, the proposed device can nearly realize a  $2\pi$  phase shift at both frequencies. Note that, the intrinsic loss of graphene limits the phase shift range. Based on the results in Fig. 2(a) and (b), the appropriate Fermi levels of graphene ribbons can be chosen easily. To better illustrate the origin of these two resonances, the normalized intensity distributions are simulated at two resonant frequencies and shown in Fig. 2(c). When the Fermi levels of two layers graphene are set as the same as 0.26 eV, the interaction between light and graphene will take place at both graphene layers. It is an intrinsic disadvantage for manipulating the incident waves. Therefore, we should separately tune the Fermi levels of graphene ribbons to individually implement responses of the graphene layer. To this end, we set the Fermi level of top and bottom graphene ribbon as 0.73 eV and 0.26 eV, respectively. Under normal incidence at 3.5 THz, there is a significant field enhancement at the bottom graphene ribbons, while the near field is barely enhanced the top graphene ribbons, as shown in Fig. 2(d). In contrast, under normal incidence at 7.0 THz, the electric field is significant enhanced near the top graphene ribbons, while is not clearly enhanced at the bottom graphene ribbons, as shown in Fig. 2(e). It is further demonstrated that the interaction between the two resonances is very small. Therefore, we can choose 3.5 THz and 7.0 THz as the working frequencies.

To demonstrate the validity of the proposed devices, we have designed tunable dual-band terahertz metalens working at 3.5 THz and 7 THz simultaneously. Under normal conditions, the traditional parabolic reflectors can converge incident plane wave at arbitrary points in free space according to the phase distribution along the reflector surface. For planar graphene metalens, the graphene metasurface can modulate the needed phase of the reflected light by the concrete Fermi level's modulation, so that the reflected light can also be focus in a point.

The parabolic phase profile along the metasurface is given by the expression:

$$\varphi(x) = \frac{2\pi}{\lambda_0} \left( \sqrt{F^2 + (x - \Delta x)^2} - F \right) \quad (5)$$

where  $\lambda_0$  is the incident wavelength,  $F$  is the focal length and  $x$  is the position of graphene ribbons,  $\Delta x$  is the horizontal offset of the focal point from the center. According to Fig. 2(a) and (b), we can determine the Fermi levels of graphene ribbons along metasurface to match the phase profiles. For the phase modulations locating in the blank range of phase modulations, we just employ graphene ribbons with the approximate Fermi level in the real designing processes. To evaluate the focusing ability, numerical aperture (NA) is also calculated by:

$$NA = \sin \left[ \tan^{-1} (D/2F) \right] \quad (6)$$

where  $D$  is the width of graphene metasurface. In our work,  $D = 940 \mu\text{m}$ , the focal length of the bottom and top graphene metasurface is set as  $F = 300 \mu\text{m}$  and  $100 \mu\text{m}$ , the NA can be calculated as 0.84 and 0.98, respectively.

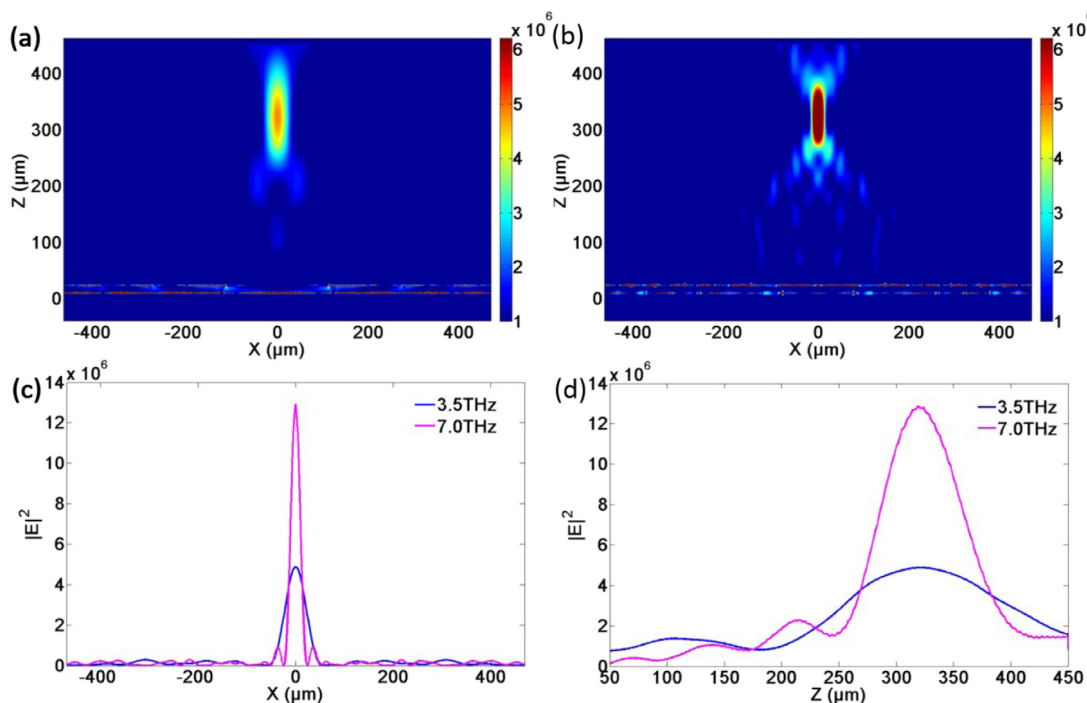


Fig. 3. Intensity distributions of reflective focusing waves from the same metasurface designed under the normal incidences at (a) 3.5 THz, (b) 7.0 THz. The intensity distributions along the (c) X direction and (d) Z direction at different frequencies.

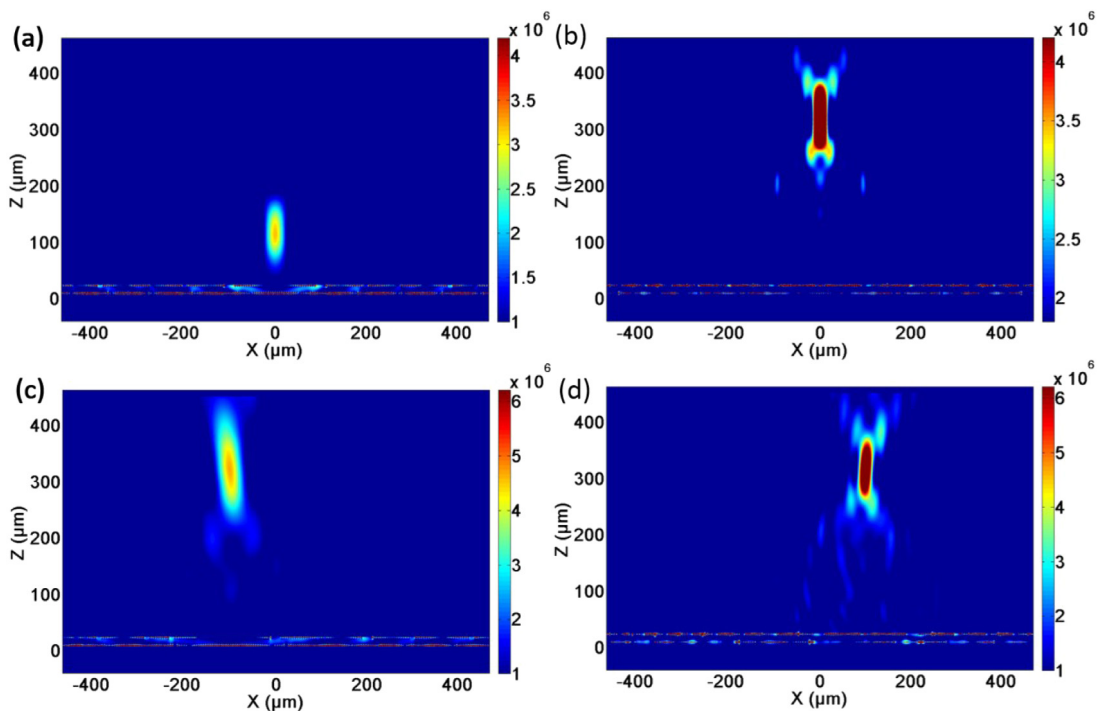


Fig. 4. Intensity distributions of lens based on graphene metasurface with the different focusing lengths at the working frequency of (a) 3.5 THz and (b) 7.0 THz. Off-axis focusing grapheme metasurface at the working frequency of (c) 3.5 THz incidence with  $\Delta x = -100 \mu\text{m}$  and (d) 7.0 THz incidence with  $\Delta x = 100 \mu\text{m}$ .

Based on the above results, we design a dual-band terahertz metalens based on stacked graphene metasurfaces, working at both 3.5 THz and 7 THz. The focal length of both operating frequencies is  $f = 300 \mu\text{m}$  with  $\Delta x = 0$ . The corresponding Fermi levels of graphene ribbons at the top and bottom layers are obtained directly according to the results in Fig. 2(a) and (b). The simulation result of the designed focusing lens at 3.5 THz and 7.0 THz is shown in Fig. 3(a) and (b), respectively.

When TM polarized plane waves are normally incident to the graphene metasurface, the energy will be tightly focused at  $320 \mu\text{m}$  for both 3.5 THz and 7.0 THz. Considering the finite thickness of metasurface, the simulation result is in a good agreement with the theoretical values. Fig. 3(c) and (d) show the intensity of the focusing spots at frequencies of both 3.5 THz and 7.0 THz along x- and z-direction, respectively. The focusing resolution of the designed metasurface (full width at half

maximum along  $x$ -direction) are 48.2  $\mu\text{m}$  and 21.5  $\mu\text{m}$  at frequency of 3.5 THz and 7.0 THz, respectively. The resolutions are close to half of the corresponding incident wavelengths, demonstrating a high performance of the designed metasurface. As shown in Fig. 3(d), the depths of focus (full width at half maximum along  $z$ -direction) are 174.7  $\mu\text{m}$  and 84  $\mu\text{m}$  for the focusing lenses with the working frequencies of 3.5 THz and 7.0 THz, respectively. Overall, the above results demonstrate that our designed graphene metasurface has superior performances.

To further demonstrate its applicability, we design a metasurface to focus light with different frequencies at different position. Thus, the stacked graphene composing the designed metasurface needs to be dynamically tuned. Based on the results above, we designed a stacked graphene metasurface to focus incident plane wave with frequency of 3.5 THz and 7.0 THz at focal length of 100  $\mu\text{m}$  and 300  $\mu\text{m}$ , respectively. Fig. 4(a) and (b) shows the intensity distribution of reflective focusing at frequency of 3.5 THz and 7.0 THz, respectively. When the phase distribution of the bottom graphene ribbons is changed by applying different gate voltages, the focal length of graphene metasurface can be adjusted to 100  $\mu\text{m}$  and 300  $\mu\text{m}$  when the incident light is 3.5 THz and 7.0 THz, respectively.

In addition to the common parabolic reflectors, the graphene metasurface can not only change the focal length, but also achieve a lateral shift of focus. As shown in Fig. 4(c) and (d), the stacked graphene metasurfaces have same focal length but different offset distances ( $\Delta x = -100 \mu\text{m}$  for 3.5 THz incidence and  $\Delta x = 100 \mu\text{m}$  same focal length at two different working frequencies can also be achieved with specific offsets. These results demonstrate that our designed graphene metasurface has superior performances in the tunability.

### 3. Conclusions

In summary, we have systematically studied the control of phase and amplitude of the terahertz waves by designing tunable stacked graphene metasurface, where different Fermi levels of graphene ribbons can be independently designed at two distinct working frequencies of 3.5 and 7.0 THz. Based on this configuration, a practical function of tunable dual-band terahertz metalens is designed and numerically demonstrated. In addition, the resolution of focusing spots (full width at half maximum along the  $x$ -direction) of the designed lens are close to the half of incident wavelengths. In addition, the focal length and offset distance of focal point of the designed metalens can be tuned by changing gate voltages on the graphene ribbons. The designed stacked graphene metasurface has great potentials for tunable, multifunctional, multiband devices and integrated optoelectronic regions.

### Funding

The authors gratefully acknowledge the financial supports for this work from the National Natural Science Foundation of China (61775050, 61571175), Natural Science Foundation of Anhui Province, China (1808085MF188, 1808085QA21), Science and Technology Planning Project of Guangdong Province, China (2016B010108002), Fundamental Research Funds for the Central Universities, China (JD2017JGPY0005), State Key Laboratory of Millimeter Waves, China (K2017111).

### References

- N. Yu, Z. Gaburro, Light propagation with phase discontinuities: generalized laws of reflection and refraction, *Science* 334 (6054) (2011) 333.
- C.L. Holloway, E.F. Kuester, J.A. Gordon, et al., An overview of the theory and applications of metasurfaces: The two-dimensional equivalents of metamaterials, *IEEE Antennas Propag. Mag.* 54 (2) (2012) 10–35.
- N. Yu, F. Capasso, Flat optics with designer metasurfaces, *Nature Mater.* 13 (2) (2014) 139–150.
- F. Monticone, N.M. Estakhri, A. Alù, Full control of nanoscale optical transmission with a composite metascreen, *Phys. Rev. Lett.* 110 (20) (2013) 20393.
- X. Ni, N.K. Emani, A.V. Kildishev, et al., Broadband light bending with plasmonic nanoantennas, *Science* 335 (6067) (2012) 427–427.
- L. Huang, X. Chen, B. Bai, et al., Helicity dependent directional surface plasmon polariton excitation using a metasurface with interfacial phase discontinuity, *Light: Sci. Appl.* 2 (3) (2013) e70.
- J. Lin, J.P. Mueller, Q. Wang, et al., Polarization-controlled tunable directional coupling of surface plasmon polaritons, *Science* 340 (6130) (2013) 331.
- Z. Guo, Z. Li, J. Zhang, K. Guo, F. Shen, Q. Zhou, H. Zhou, Review of the functions of archimedes' spiral metallic nanostructures, *Nanomaterials* 7 (2017) 405.
- R. Li, Z. Guo, W. Wang, et al., Arbitrary focusing lens by holographic metasurface, *Photonics Res.* 3 (5) (2015) 252–255.
- A. Pors, M.G. Nielsen, R.L. Eriksen, et al., Broadband focusing flat mirrors based on plasmonic gradient metasurfaces, *Nano Lett.* 13 (2) (2013) 829–834.
- Z. Guo, H. Xu, K. Guo, F. Shen, H. Zhou, Q. Zhou, J. Gao, Z. Yin, High-efficiency visible transmitting polarizations devices based on the gan metasurface, *Nanomaterials* 8 (2018) 333.
- T. Niu, W. Withayachumnankul, A. Upadhyay, et al., Terahertz reflectarray as a polarizing beam splitter, *Opt. Express* 22 (13) (2014) 16148–16160.
- Z. Guo, L. Zhu, K. Guo, et al., High-order dielectric metasurfaces for high-efficiency polarization beam splitters and optical vortex generators, *Nanoscale Res. Lett.* 12 (1) (2017) 512.
- N. Yu, F. Aieta, P. Genevet, et al., A broadband, background-free quarter-wave plate based on plasmonic metasurfaces, *Nano Lett.* 12 (12) (2012) 6328.
- R. Li, Z. Guo, W. Wang, et al., High-efficiency cross polarization converters by plasmonic metasurface, *Plasmonics* 10 (5) (2015) 1167–1172.
- S. Khatua, W.S. Chang, P. Swanglap, et al., Active modulation of nanorod plasmons, *Nano Lett.* 11 (9) (2011) 3797.
- N.H. Shen, M. Massoufi, M. Gokkavas, et al., Optically implemented broadband blueshift switch in the terahertz regime, *Phys. Rev. Lett.* 106 (3) (2011) 037403.
- T.F. Zhang, Z.P. Li, J.Z. Wang, et al., Broadband photodetector based on carbon nanotube thin film/single layer graphene Schottky junction, *Sci. Rep.* 6 (2016) 38569.
- W.Y. Kong, G.A. Wu, K.Y. Wang, et al., Graphene- $\beta$ -Ga2O3 heterojunction for highly sensitive deep UV photodetector application, *Adv. Mater.* 28 (48) (2016) 10725–10731.
- A. Vakil, N. Engheta, Transformation optics using graphene, *Science* 332 (6035) (2011) 1291–1294.
- F.H.L. Koppens, D.E. Chang, F.J. Garcia de Abajo, Graphene plasmonics: a platform for strong light–matter interactions, *Nano Lett.* 11 (8) (2011) 3370–3377.
- L. Ju, B. Geng, J. Horng, et al., Graphene plasmonics for tunable terahertz metamaterials, *Nature Nanotechnol.* 6 (10) (2011) 630–634.
- Liming Liu, Yair Zaraté, Haroldo T. Hattori, Dragomir N. Neshev, Ilya V. Shadrivov, David A. Powell, Terahertz focusing of multiple wavelengths by graphene metasurfaces, *Appl. Phys. Lett.* 108 (2016) 031106.
- W. Ma, Z. Huang, X. Bai, et al., Dual-band light focusing using stacked graphene metasurfaces, *ACS Photonics* 4 (7) (2017) 1770–1775.
- L. Wang, X. Chen, A. Yu, et al., Highly sensitive and wide-Band tunable terahertz response of plasma waves based on graphene field effect transistors, *Sci. Rep.* 4 (2014) 5407.
- W. Tang, L. Wang, X. Chen, et al., Dynamic metamaterial based on the graphene split ring high-Q Fano-resonator for sensing applications, *Nanoscale* 33 (8) (2016) 151–196.
- V.P. Gusynin, S.G. Sharapov, J.P. Carbotte, Magneto-optical conductivity in Graphene. (2007) 19(2): 249–264.
- P.Y. Chen, A. Alù, Atomically thin surface cloak using graphene monolayers, *ACS Nano* 5 (7) (2011) 5855.
- Z.Q. Li, E.A. Henriksen, Z. Jiang, et al., Dirac charge dynamics in graphene by infrared spectroscopy, *Nat. Phys.* 4 (7) (2008) 532–535.
- G.W. Hanson, Quasi-transverse electromagnetic modes supported by a graphene parallel-plate waveguide, *J. Appl. Phys.* 104 (8) (2008) 084314.
- H. Cheng, S. Chen, P. Yu, et al., Dynamically tunable broadband infrared anomalous refraction based on graphene metasurfaces, *Adv. Opt. Mater.* 3 (12) (2015) 1744–1749.
- A. Ishikawa, T. Tanaka, Plasmon hybridization in graphene metamaterials, *Appl. Phys. Lett.* 102 (25) (2013) 253110.
- L. Luo, K. Wang, C. Ge, et al., Actively controllable terahertz switches with graphene-based nongroove gratings, *Photonics Res.* 5 (6) (2017) 604.
- K.S. Novoselov, A.K. Geim, S.V. Morozov, et al., Electric field effect in atomically thin carbon films, *Science* 306 (2004) 666–669.
- A. Vakil, N. Engheta, Transformation optics using graphene, *Science* 332 (6035) (2011) 1291.
- L. Luo, K. Wang, K. Guo, et al., Tunable manipulation of terahertz wavefront based on graphene metasurfaces, *J. Opt.* 19 (11) (2017) 115104.
- F.H.L. Koppens, D.E. Chang, F.J. Garcia de Abajo, Graphene plasmonics: a platform for strong light–matter interactions, *Nano Lett.* 11 (8) (2011) 3370–3377.
- M. Furchi, A. Urich, A. Pospischil, et al., Microcavity-integrated graphene photodetector, *Nano Lett.* 12 (6) (2012) 2773–2777.
- J. Ding, B. Arigong, H. Ren, et al., Mid-infrared tunable dual-frequency cross polarization converters using graphene-based L-shaped nanoslotarray, *Plasmonics* 10 (2) (2015) 351–356.